



Excitation and ionic fragmentation of the carvone molecule ($C_{10}H_{14}O$) around the O 1s edge

R.B. de Castilho ^{a,*}, C.V. Nunez ^b, A.F. Lago ^c, A.C.F. Santos ^d, L.H. Coutinho ^d, C.A. Lucas ^e, S. Pilling ^f, M.O. Silva-Moraes ^a, G.G.B. de Souza ^g

^a Departamento de Química, Instituto de Ciências Exatas, Universidade Federal do Amazonas (UFAM), Campus Universitário, Coroado, 69077-000 Manaus, AM, Brazil

^b Coordenação de Pesquisas em Produtos Naturais, Instituto Nacional de Pesquisas da Amazônia, INPA, 69060-001 Manaus, AM, Brazil

^c Centro de Ciências Naturais e Humanas, Universidade Federal do ABC (UFABC), 09210-170 Santo André, SP, Brazil

^d Instituto de Física, Universidade Federal do Rio de Janeiro, Caixa Postal 68528, 21941-972 Rio de Janeiro, RJ, Brazil

^e Instituto de Química, Universidade Federal Fluminense (UFF), 24020150 Rio de Janeiro, Brazil

^f Instituto de Pesquisa e Desenvolvimento (IP&D), Universidade do Vale do Paraíba (UNIVAP), 12244-000 São José dos Campos, SP, Brazil

^g Instituto de Química, Universidade Federal do Rio de Janeiro (UFRJ), Cidade Universitária, Ilha do Fundão, 21949-900 Rio de Janeiro, RJ, Brazil



ARTICLE INFO

Article history:

Received 29 November 2013

Received in revised form 22 January 2014

Accepted 24 January 2014

Available online 3 February 2014

Keywords:

Carvone

Synchrotron radiation

Time of flight

Mass spectrometry

ABSTRACT

The electronic excitation and associated ionic dissociation of the carvone molecule have been studied around the oxygen 1s edge, using synchrotron radiation and time-of-flight techniques. Photoabsorption spectrum (total ion yield) and mass spectra have been obtained in the range between 520 and 545 eV. For the sake of comparison, carvone mass spectra have also been obtained following valence (21.21 eV) and core (carbon 1s) ionization. Fragmentation of the molecule is seen to be greatly enhanced following core excitation. Around the oxygen 1s edge, we observe an extensive fragmentation of the molecular skeleton, as exemplified by the appearance of several previously unreported ions: H^+ , H_2^+ , CH^+ , CH_2^+ and CH_3^+ , which are not formed at low energies. A maximum is observed at 536 eV photon energy in the relative intensity of the oxygen-containing ions O^+ , O^{2+} and OH^+ , as an evidence for the existence of site-selective fragmentation of the carvone molecule excited around the O 1s edge. Absolute values for the photoionization and photodissociation cross sections were estimated using the molecular additive rule.

© 2014 Elsevier B.V. All rights reserved.

1. Introduction

The interaction of a molecule with soft X-ray photons (arbitrarily defined here as photons with energy greater than 100 eV) basically results in the ejection of one or more electrons. In fact, while in most molecules the first ionization potential (IP) occurs at less than 15 eV, the direct double ionization potential is usually of the order of 30–40 eV and the triple ionization potential is of the order of 50–80 eV [1,2]. Although strictly forbidden in an independent particle model, double and triple ionization become possible through electron correlation and shake-off type processes. Around the edges of core-shell electrons, additional photoabsorption processes come into play, namely the excitation and ionization of inner-shell electrons. For molecules built with light atoms, the main relaxation mechanism, following photon absorption, is Auger decay. Below the ionization edge, transitions to unoccupied elec-

tronic states will be followed by autoionization-type processes and one or more electrons will be emitted by the molecule. In these so-called resonant Auger processes, the excited electron may remain either as spectator or participant in the relaxation decay mechanism. In the first case (spectator resonant Auger), and assuming the ejection of a single valence electron, the final state will be that of an excited ion. When the excited electron participates in the electronic decay (participating resonant Auger), the final state will be a singly charged ion, indistinguishable in principle from the final state associated with a simple valence shell ionization of the molecule. Above the core ionization edge, Auger decay involves the ejection of one (or more) valence-shell electrons and the final state will be a doubly, triply, etc., cation. The stability of the remaining ion, in all cases, will very much depend on the nature (bonding, antibonding, Rydberg) of the depleted valence orbital and electronic state. Doubly or multiply charged ions will in general have a more unstable nature, due to coulomb repulsion and to the possible loss of bonding electrons, resulting in ionic states highly dissociative. The large energy gap between the ionization edges of different atoms and the availability of tunable synchrotron radiation allows

* Corresponding author. Tel.: +55 09233052870.

E-mail addresses: bobcast@gmail.com, rccastilho@ufam.edu.br (R.B. de Castilho).

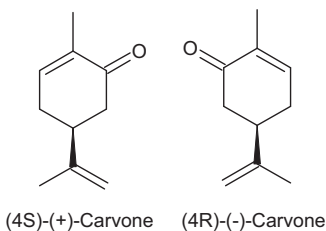


Fig. 1. Chemical structures of the carvone isomers.

for the excitation of different sites in a given molecule. As a consequence, site-selective fragmentation may be sometimes observed [3,4]. With ionic dissociation processes prevailing after the interaction of molecules with high energy photons, mass spectrometric techniques have become very useful toward the understanding of the relaxation mechanisms associated with high energy photon absorption.

In this respect, time-of-flight techniques (mass spectrometry, electron-ion and electron-ion-ion techniques) are known as powerful tools for the elucidation of the dissociation mechanisms of highly excited molecules. Excellent reviews about the photoionization of molecules and the use of time-of-flight techniques may be found in the literature [5–7].

We have recently started a systematic study of the core excitation and ionic dissociation of molecules of biological interest, in the gas phase, focusing mainly in aminoacids [8,9], nucleic acid bases [10,11] and volatile natural products [12,13]. In this paper, we present and discuss new experimental results related to a volatile natural product, carvone ($C_{10}H_{14}O$), excited at valence and around the C 1s and O 1s edges. Carvone is an enantiomeric substance found in plants like caraway, dill and spearmint (Fig. 1). The antimicrobial activity of the carvone isomers has been demonstrated against a wide spectrum of human pathogenic fungi and bacteria [14]. The amount of mentha essential oil, which contains appreciable quantities of carvone, is suppose to be associated with the incidence of UV-B radiation, reflecting, probably, a defense mechanism [15]. The carvone molecule is chemically classified as a monoterpene (C_{10}), consisting of an unsaturated cyclic ketone with methyl and isopropenyl substitution in opposite (equatorial) positions. The carvone present in essentials oils is a mixture of three conformers, differing in respect to the bond connecting the ring and the isopropenyl moiety [16]. The first systematical study of monoterpenes ketones and aldehydes, employing gas chromatography and mass spectrometry [using 20 eV electrons], was published in 1964 [17]. Recently, the mass spectrum and threshold photoelectron spectrum of carvone has been studied in the 8–11 eV photon energy range. It was pointed out that the HOMO orbital in carvone is associated with the oxygen atom lone pair, essentially localized around the carbonyl group, with an ionization potential of 8.7 eV [18]. The circular dichroism of the carvone enantiomers, randomly oriented in gas-phase, has also been investigated both theoretically and using circularly polarized synchrotron radiation at the C 1s edge [19,20]. In our present study, we have recorded electron-ion coincidence (PEPICO) and total ion yield (TIY) spectra for the carvone molecule. The PEPICO spectra were obtained below (520 eV), around (530–540 eV) and above (545 eV) the O 1s edge, which is arbitrarily taken to occur at 540 eV. For the sake of comparison, PEPICO spectra were also obtained following valence ionization (21.21 eV) and before (275 eV) and above (310 eV) the C 1s edge, which is arbitrarily taken to occur at 290 eV. Compared to valence excitation, it is well known that core excitation usually induces a much larger degree of fragmentation of the molecule. In particular, fragments such as O^+ and O^{2+} are observed only around the O 1s

edge, pointing out to possible site-selective fragmentation mechanisms.

2. Experiment

The experiment was performed at the Laboratório Nacional de Luz Síncrotron (LNLS), Campinas, Brazil. The experimental set up has been previously described in details [21,22]. Briefly, light from a toroidal grating monochromator (TGM) (12–310 eV) and spheroidal grating monochromator (SGM) (300–1000 eV) bending magnet beamlines intersects the effusive vapor sample inside a high vacuum chamber, with base pressure in the 10^{-8} Torr range. During the experiment, the pressure was maintained below 10^{-5} Torr. The emergent beam was recorded by a light sensitive diode. The ionized fragments produced by the interaction of the gaseous sample with the light beam are accelerated by a two-stage electric field and detected by a pair of micro-channel plate detectors mounted in a chevron configuration. The ions produce stop signals to a time-to-digital converter (TDC). Electrons, accelerated in an opposite direction with respect to the positive ions, are recorded without energy analysis by two micro-channel plate detectors and provide the start signal to the TDC. A 708 V/cm DC electric field is applied to the first ion acceleration stage. The time-of-flight spectrometer was designed in order to achieve 100% efficiency for ions with kinetic energies up to 30 eV. The electrons produced in the ionization region are focused by an electrostatic lens designed to focus them at the center of the micro-channel plate detector. The bias voltages are applied in order to not vary the relative intensity between different masses. The detector efficiency determined near the C 1s threshold for the CO molecules is of 0.29 for the detection of a single ion [23]. All electrons with kinetic energy up to 150 eV are detected without angular discrimination. Negative ions may also be produced and detected, but the corresponding cross sections are considered to be negligible. The sample of R-(−)-carvone was purchased from Sigma-Aldrich with a purity of 98% and was used without further purification. The carvone sample is a liquid at ambient pressure and temperature. In order to avoid sample condensation, the inlet system was kept at 45 °C.

3. Results and discussion

3.1. Valence-shell and C 1s ionization

The photoionization mass spectrum of the carvone molecule measured at 21.21 eV with a He I discharge lamp is shown in Fig. 2, and the corresponding branching ratios for the ionic fragments is

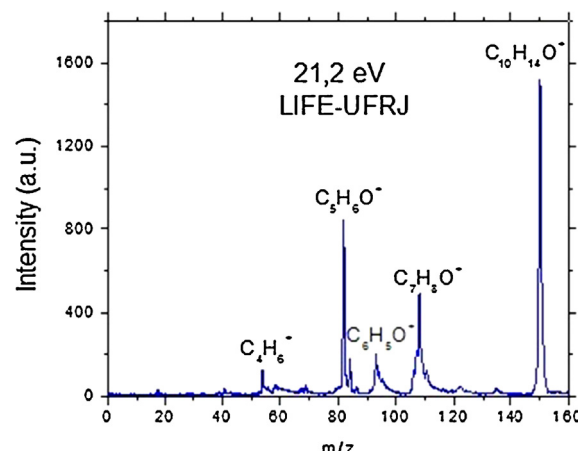


Fig. 2. Mass spectrum of the carvone molecule obtained at 21.21 eV with a He I discharge lamp.

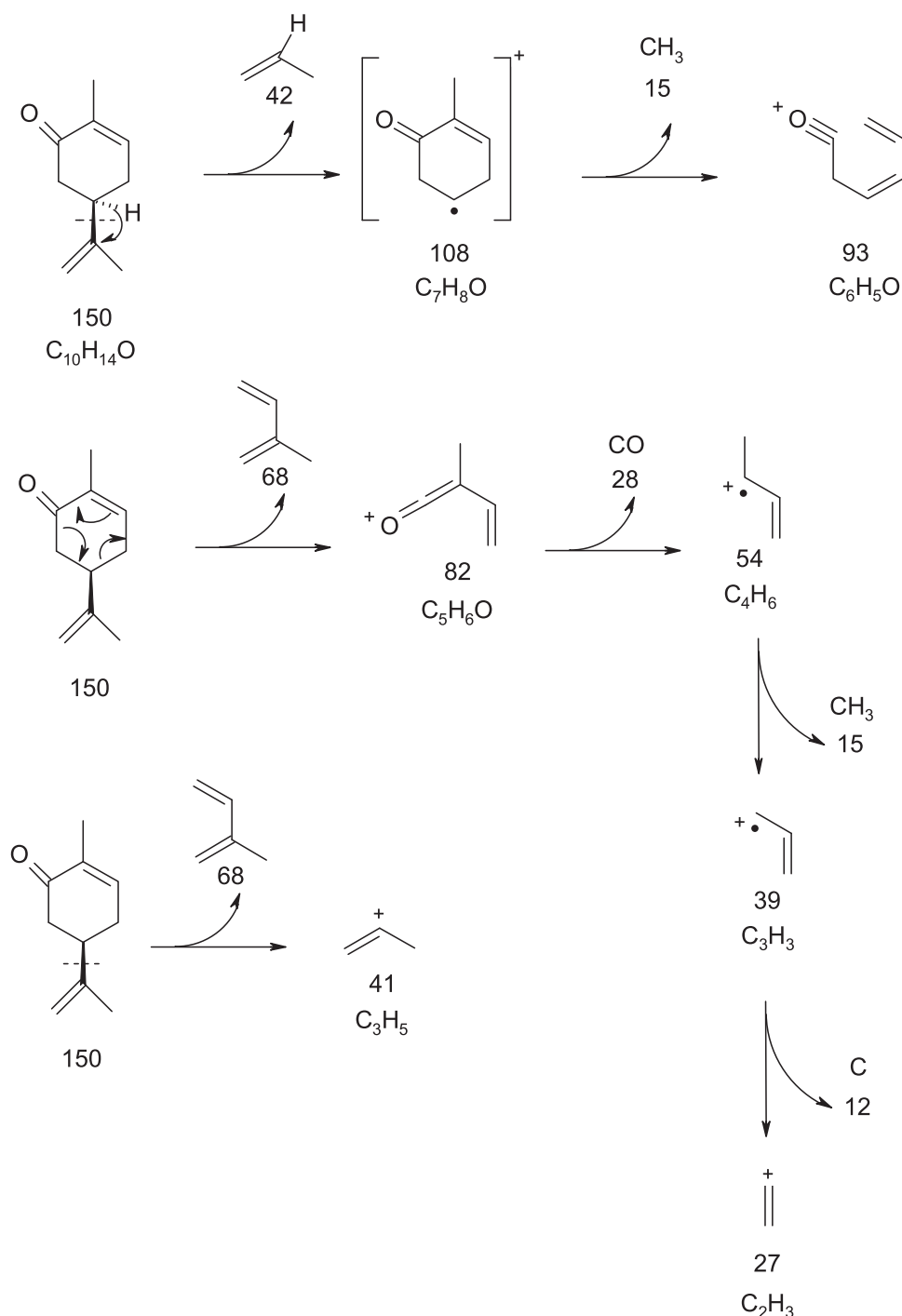


Fig. 3. Proposed mechanisms for the fragmentation of the carvone parent ion.

presented in Table 1. The associated error is estimated to be 10%. The base peak corresponds to the parent ion, $\text{C}_{10}\text{H}_{14}\text{O}^+$ ($m/z = 150$). Other prominent peaks correspond to the following m/z values: 108 ($\text{C}_7\text{H}_8\text{O}^+$), 93 ($\text{C}_6\text{H}_5\text{O}^+$), 84 ($\text{C}_5\text{H}_6\text{O}^+$), 82 ($\text{C}_5\text{H}_6\text{O}^+$) and 54 (C_4H_6^+). This is at variance with respect to the known electron impact mass spectrum, not shown here, usually obtained at 70 eV [24]. In the electron impact spectrum, we observe a larger degree of fragmentation as compared to the spectrum obtained with a He I lamp. Indeed, in the electron impact mass spectrum the base peak corresponds to the $\text{C}_5\text{H}_6\text{O}^+$ ion ($m/z = 82$), and not to the parent ion ($m/z = 150$). Other ions are also observed, albeit with low intensity: 41 (C_3H_5^+) and 39 (C_3H_3^+). In Fig. 3, we present some proposed

coherent mechanisms for the fragmentation of the carvone parent ion. The first diagram involves the breakage of the isopropenyl moiety, producing the $\text{C}_7\text{H}_8\text{O}^+$ ($m/z = 108$) ion, followed by the loss of methyl radical to produce the $\text{C}_6\text{H}_5\text{O}^+$ ($m/z = 93$) ion. The second mechanism involves a retro Diels Alder reaction to produce the $\text{C}_5\text{H}_6\text{O}^+$ ($m/z = 82$) ion – the corresponding base peak in the electron impact mass spectrum – followed by the loss of carbon monoxide to produce the C_4H_6^+ ($m/z = 54$) ion.

The carbon 1s binding energies are 292.8 eV (carbonyl), 290.5 eV (mean carbon–hydrogen bond) and 289.8 eV (carbon–carbon double bond) according to Harding et al. [20]. The photoionization mass spectra obtained before (275 eV) and above (310 eV) the C 1s edge

Table 1

Branching ratios (%) for the most intense ions as function of photon energy. The related uncertainties are around 10%.

m/z	Assignment	He-I	Synchrotron radiation	
		21.21 eV	275 eV	310 eV
1	H ⁺	–	0.282	0.87
2	H ₂ ⁺	–	–	0.13
12	C ⁺	–	–	0.17
15	CH ₃ ⁺	–	1.27	2.58
27	C ₂ H ₃ ⁺	–	4.74	7.23
39	C ₃ H ₃ ⁺	–	13.4	11.2
54	C ₄ H ₆ ⁺	1.83	4.29	3.6
82	C ₅ H ₆ O ⁺	3.77	13.7	10.5
84	C ₅ H ₈ O ⁺	3.17	–	–
93	C ₆ H ₅ O ⁺	3.77	3.53	7.01
108	C ₇ H ₈ O ⁺	8.4	2.26	1.75
152	C ₁₀ H ₁₄ O ⁺	47.4	6.22	3.86

spectra are presented in Fig. 4. In both spectra, we observe an extensive fragmentation of the molecule, giving rise to lighter ions: C₄H₆⁺ (*m/z* = 54), C₃H₃⁺ (*m/z* = 39), C₂H₃⁺ (*m/z* = 27), CH₃⁺ (*m/z* = 15), H⁺ (*m/z* = 1). In Fig. 3, we have presented mechanisms to produce some of these lighter ions. The relative intensity of the parent ion C₁₀H₁₆O⁺ (*m/z* = 150) is smaller when compared to the valence spectrum previously discussed. The base peak (Fig. 4) corresponds to the C₅H₆O⁺ (*m/z* = 82) ion, as equally observed in the electron impact mass spectrum. At 310 eV photon energy, Auger processes will give rise to highly dissociative doubly (or triply) ionic states and fragmentation of the molecule increases, resulting in high abundances of lighter ionic fragments. We observe the production of the C⁺ (*m/z* = 12) ion, pointing out to the atomization of the molecular skeleton. A small peak at *m/z* = 2 (H₂⁺), resulting from a molecular rearrangement, can also be observed. The branching ratios (BR) for the most intense ions formed at 21.21, 275 and 310 eV photon energies are presented in Fig. 5. The relative intensities of heavier ionic fragments decrease with increasing photon energy, while the opposite behavior is observed for the lighter ones. Interestingly, the C₅H₆O⁺ (*m/z* = 82) ion corresponds to the base peak at 310 eV and to the second most intense peak at the 21.21 eV mass spectrum, suggesting a considerable structural and energetic stability.

A similar study, conducted within the same experimental conditions, has shown that another monoterpene, limonene, also presents a very intense ionic fragmentation at high photon energies [12].

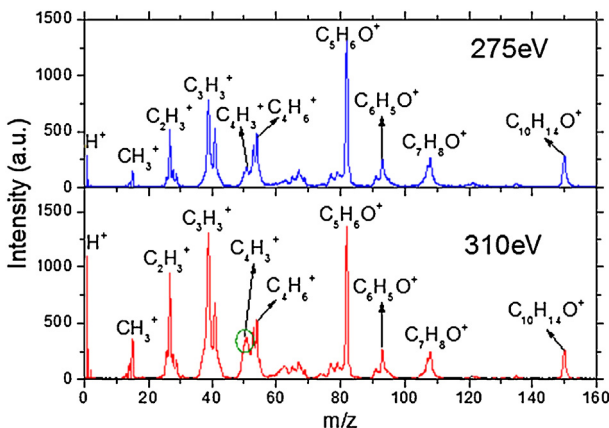


Fig. 4. Mass photoionization spectra of the carvone molecule obtained at 275 and 310 eV.

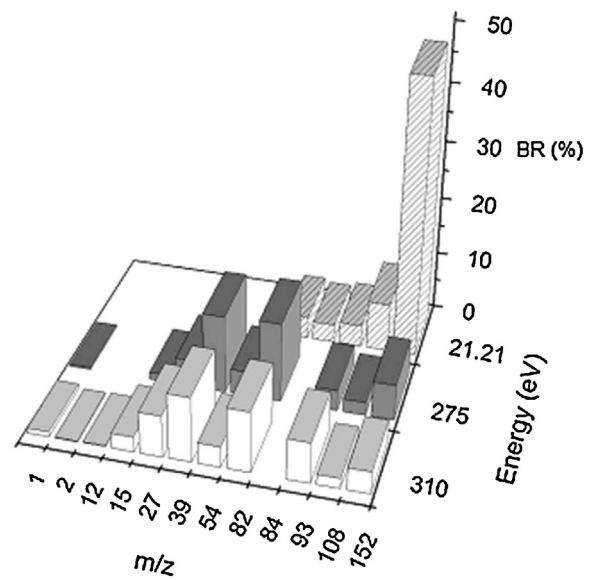


Fig. 5. Branching ratios of the PEPICO mass spectra at 21.21, 275 and 310 eV.

3.2. O 1s ionization

The total ion yield (TIY) spectrum of the carvone molecule, obtained around the O 1s edge (525–555 eV), is shown in Fig. 6. The spectrum was energy-calibrated with respect to the TIY spectrum of the O₂ molecule, obtained at the same experimental conditions, using a peak centered at about 531 eV and related to the O 1s → 1π_g* transition [25]. Three intense bands, A (531 eV), B (534 eV) and C (536 eV) are observed below the ionization edge, which, in the absence of previous measurements or calculations and by analogy with the 2-propenal molecule [26], is considered to occur at approximately 538 eV. Considering the O 1s electronic spectra of other ketones, carboxylic acids and esters well described in literature, three resonances are expected to show up below the ionization potential [26,27]. For example, the first (530.59 eV) and second (533.57 eV) bands in the 2-propenal electron energy loss spectrum (obtained under dipole-allowed conditions) involve electronic transitions to the pi-antibonding orbitals while the third one (535.25 eV) involves a mixture of 3p-sigma and 3p-pi states. Close to the O 1s edge (538 eV) a convolution of Rydberg states are normally observed. Above the ionization edge, an intense and

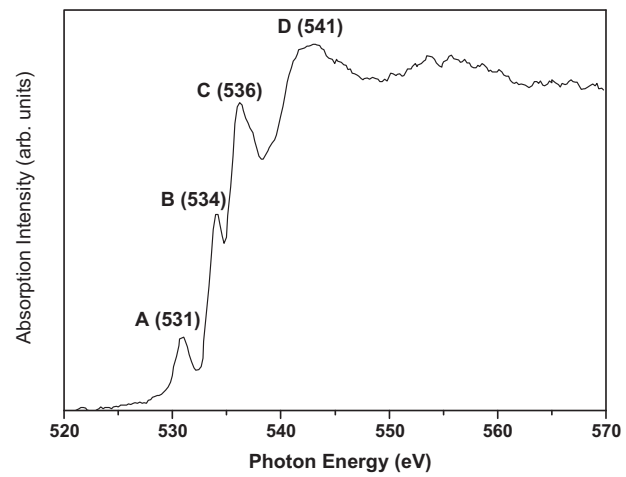


Fig. 6. Total ion yield (TIY) spectrum of the carvone molecule measured around the O 1s edge, highlighting the main resonances.

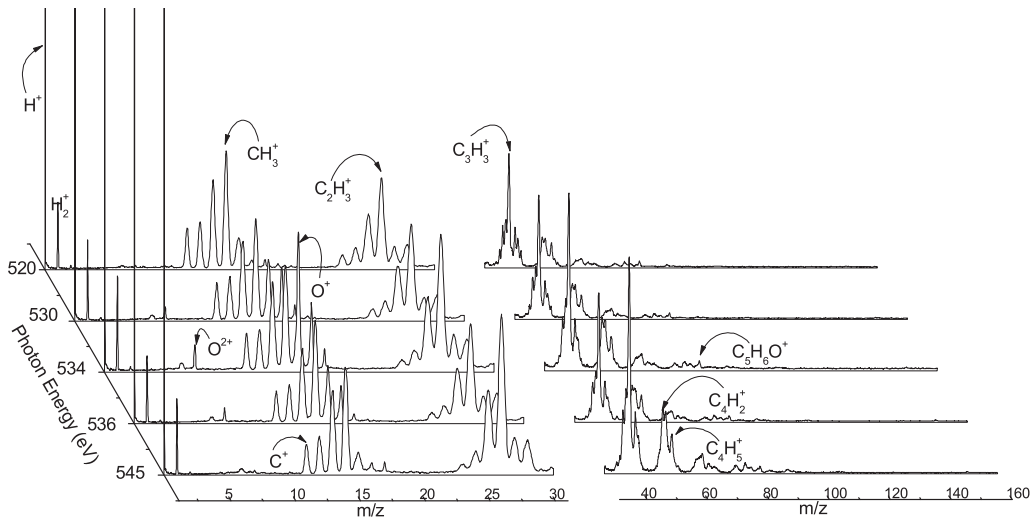


Fig. 7. Mass spectra of the carvone molecule around the O 1s edge.

broad structure, D (541 eV), is observed and could be in principle assigned to an antibonding sigma shape resonance. The mass spectra obtained at 520 eV, 531 eV, 534 eV, 536 eV and 545 eV are presented in Fig. 7. The very low intensity peaks correspond to heavier fragments. In our spectra, only the peaks corresponding to ions with m/z lower than 82 are presented. The five spectra are similarly dominated by light ionic fragments pointing out to an extensive molecular fragmentation. A complete and representative mass spectrum for the carvone molecule, obtained at 536 eV is shown in Fig. 8. The inset on the right hand side of the figure helps visualization of the CH_n^+ , O^+ , OH^+ and H_2O^+ ions, while in the inset on the left hand side, we confirm the production of H_3^+ , CH_2^{2+} and O^{2+} ions. The parent ion is not observed in the mass spectra measured around the O 1s edge.

As the photon energy gets closer to the O 1s edge, a significant relative intensity increase is observed for peaks with low m/z values such as H^+ ($m/z=1$), H_2^+ ($m/z=2$), H_3^+ ($m/z=3$) and CH_2^{2+} ($m/z=7$). The H_3^+ ion is very important from an astrophysical point of view and has already been observed in a similar experiment [21]. Both H_2^+ and H_3^+ are produced with very low relative intensities.

The appearance of peaks at $m/z=8$ (O^{2+}) and $m/z=16$ (O^+), not observed at lower photon energies, can be seen as a signature of a site-selective fragmentation around the O 1s edge. Site selectivity in

the fragmentation of core-excited molecules was first described by Eberhardt et al. [3]. The branching ratios for oxygen-containing ions such as O^{2+} [$m/z=8$], O^+ [$m/z=16$] and HO^+ [$m/z=17$] are presented as a function of the photon energy in Fig. 9. A maximum is observed at 536 eV for all ions, corroborating the suggestion of site-selective mechanisms.

The ionic fragments OH^+ ($m/z=17$) H_2O^+ ($m/z=18$) had not been reported before for this molecule. A group of ionic fragments can also be observed at the following m/z values: 24 [C_2^+], 25 [C_2H^+], 26 [C_2H_2^+], 27 [C_2H_3^+], 28 [C_2H_4^+ or CO^+], 29 [C_2H_5^+]. The branching ratios for the most abundant ions are presented in Table 2. The relative intensity of the H^+ [$m/z=1$] ion increases considerably from 520 eV to 531 eV, remaining almost constant between 536 and 545 eV. The relative intensity of the H_2^+ [$m/z=2$] ion remains basically constant around the O 1s edge. The relative intensity increase of H^+ and H_2^+ at high energies probably reflects the decay of multiply charged species. There is an increment in the relative intensity of the C^+ on moving from 510 eV to 520 eV photon energy. Production of the C^+ ion may be seen as a signature of the complete breakdown of the carbon skeleton, suggesting a poor stability of the carvone molecule when subjected to soft X-ray radiation. The relative abundances of the CH_n ions [$m/z=13-29$] remain practically constant from 520 eV to 545 eV, with a minimum at 536 eV in some cases.

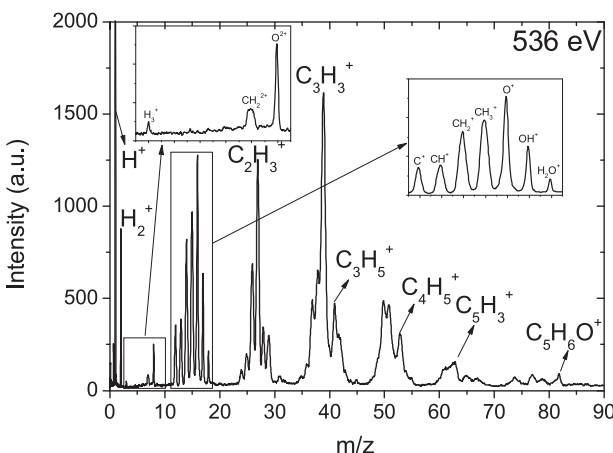


Fig. 8. Mass spectrum of the carvone molecule at 536 eV.

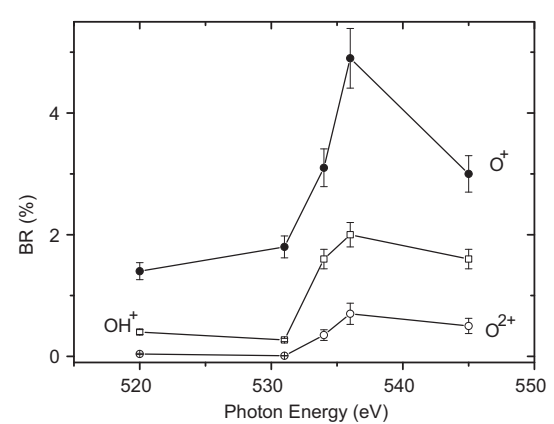


Fig. 9. Branching ratios for oxygen-containing ions around the O 1s edge.

Table 2

Branching ratios (%) for the most intense ions following the photoionization of the carvone molecule around the O 1s edge. The related uncertainties are around 10%.

<i>m/z</i>	Attribution	520 eV	531 eV	534 eV	536 eV	545 eV
1	H ⁺	23.7	31.6	38.1	36.4	36.5
2	H ₂ ⁺	2.7	2	2.3	2.2	2
3	H ₃ ⁺	0.05	0.11	0.09	0.01	0.08
7	CH ₂ ²⁺	0.26	0.1	0.13	0.3	0.3
8	O ²⁺	0.05	0.04	0.35	0.7	0.5
12	C ⁺	1.6	2.3	2	1.4	1.6
13	CH ⁺	2.1	2.8	2.5	1.7	2.1
14	CH ₂ ⁺	5.1	5.2	5.1	3.8	4.5
15	CH ₃ ⁺	6.2	6.7	6.2	4.8	6.3
16	O ⁺	1.4	1.8	3.1	4.9	3
17	HO ⁺	0.4	0.27	1.6	2	1.6
18	H ₂ O ⁺	0.2	0.27	0.26	0.43	0.26
24	C ₂ ⁺	0.6	0.7	0.57	0.35	0.43
25	C ₂ H ⁺	1.4	1.1	1.2	0.92	0.91
26	C ₂ H ₂ ⁺	5.6	3.4	4.1	3.8	3.5
27	C ₂ H ₃ ⁺	9.3	5.5	6.4	6.8	6.2
28	CO ⁺ ; C ₂ H ₄ ⁺	2.2	1.1	1.5	1.6	1.4
29	C ₂ H ₅ ⁺	2.1	1.4	1.8	1.5	1.7

3.3. Cross sections

In order to put our data on an absolute scale, the sum of the contributions from all cationic fragments was normalized, after a linear background subtraction, to an estimated absolute value for the carvone photoabsorption cross section. Taking into consideration that an experimental absolute cross section for the carvone photoabsorption around the O 1s edge is not available in the literature, we have adopted a methodology whose validity has been discussed by Ishii and Hitchcock [27]. According to this methodology, the absorption cross section for the carvone molecule may be considered, as a first approximation, to be equal to the sum of the absorption cross sections for selected molecules (methane, propene, 2-cyclohexenone). The absorption cross sections for methane, propene and 2-cyclohexenone were obtained from the COREX Database (<http://unicorn.mcmaster.ca/corex/cedb-title.html>) [28]. Due to their molecular structural similarity, the absorption cross section around the O 1s edge for the carvone molecule was considered to be similar to the absorption cross section for the 2-cyclohexenone molecule. The photoabsorption cross section for methane and propene around the O 1s edge was considered to be 1.5×10^{-21} and $3.0 \times 10^{-21} \text{ cm}^2$, respectively (roughly their absorption cross section around 280 eV). The absorption cross sections obtained with the above described methodology can be seen in Fig. 10 (around the C 1s edge) and Fig. 11 (around the O 1s edge).

Assuming now a negligible fluorescence yield [29] and a very low anionic yield, we considered that all absorbed photons lead to cationic ionizing. As a first hypothesis we considered the absorption cross section ($\sigma_{\text{ph-abs}}$) to be equal to the sum of the single (σ^+), double (σ^{++}) and triple (σ^{+++}) ionization cross sections [30,31]. Higher multiple ionization processes are considered to be negligible. Analytically, this can be written as:

$$\sigma_{\text{ph-abs}} = \sigma^+ + \sigma^{++} + \sigma^{+++} \quad (1)$$

Correcting the single ionization events spectra (PEPICO) around the O 1s edge for aborted coincidences, we have estimated an approximate 20% contribution from double ionization events with charge separation to the PEPICO spectra. Therefore, it seems reasonable to consider that the double ionization cross section corresponds roughly to 20% of the single ionization cross section. We also assume the triple ionization cross section to correspond to 2% of the single ionization cross section [21,32–34]:

$$\sigma_{\text{ph-abs}} \approx \sigma^+ + 0.2\sigma^{++} + 0.02\sigma^{+++} = 1.22\sigma^+ \quad (2)$$

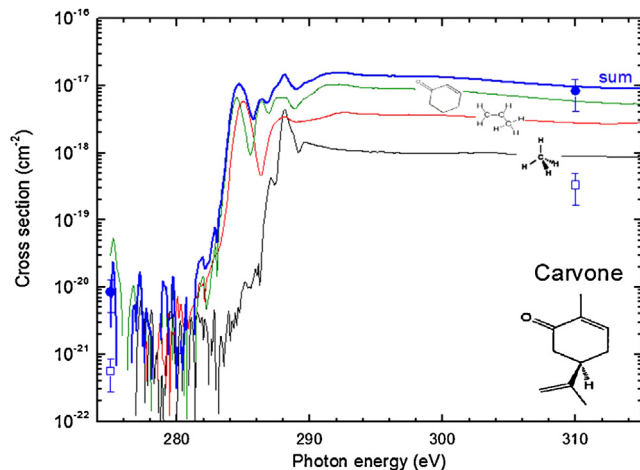


Fig. 10. Absorption cross section (lines) of selected molecules (methane, propene, 2-cyclohexenone) from COREX Database around C 1s edge. The sum of these cross section is an approximation for the carvone absorption cross section around C 1s edge. Non-dissociative single ionization (photoionization) cross section ($\sigma_{\text{ph-i}}$) and dissociative ionization (photodissociation) cross section ($\sigma_{\text{ph-d}}$) of carvone as a function of photon energy are indicated by the circles and the squares, both with error bars, respectively.

As discussed by Pilling et al. [21,35] the non-dissociative single ionization (photoionization) cross section ($\sigma_{\text{ph-i}}$) and the dissociative single ionization (photodissociation) cross section ($\sigma_{\text{ph-d}}$) of carvone can be determined by:

$$\sigma_{\text{ph-i}} = \sigma^+ \left(\frac{BR_{\text{carvone}}}{100} \right) \approx \frac{\sigma_{\text{ph-abs}}}{1.22} \left(\frac{BR_{\text{carvone}}}{100} \right) \quad (3)$$

and

$$\sigma_{\text{ph-d}} = \sigma^+ \left(1 - \frac{BR_{\text{carvone}}}{100} \right) \approx \frac{\sigma_{\text{ph-abs}}}{1.22} \left(1 - \frac{BR_{\text{carvone}}}{100} \right) \quad (4)$$

where BR_{carvone} is the branching ratio for the carvone parent ion ($C_{10}H_{14}O^+$).

From Eqs. (3) and (4), we observe that $\sigma_{\text{ph-i}} + \sigma_{\text{ph-d}} \neq \sigma_{\text{ph-abs}}$. This may be explained assuming that a fraction of incoming photons produces multiple ionizations.

The absorption cross section (lines) for the selected molecules (methane, propene, 2-cyclohexenone), obtained from the COREX Database around the C 1s edge is presented in Fig. 10. The sum of the molecular cross sections is an approximation to the carvone absorption cross section around the C 1s edge, according to the spectral sum rule [36]. The single ionization photoionization cross section and photodissociation cross section of carvone as a function of photon energy are represented by circles and the squares, respectively. The estimated total error is 50%. These values as well as the estimated values for the carvone absorption cross section ($\sigma_{\text{ph-abs}}$), obtained at 275 and 310 eV photon energy are listed in Table 3. A similar cross section determination methodology has been previously applied to derive the photodissociation and single photodissociation cross sections for the interaction of soft X-rays with benzene and methylformate [31,37].

Table 3

Non-dissociative single ionization (photoionization) cross section ($\sigma_{\text{ph-i}}$) and dissociative ionization (photodissociation) cross section ($\sigma_{\text{ph-d}}$) of carvone as a function of photon energy around the C 1s edge. Estimated values for absorption cross section ($\sigma_{\text{ph-abs}}$) of carvone are also listed. The estimated total error is 50%.

Photon energy (eV)	$\sigma_{\text{ph-d}} (10^{-19} \text{ cm}^2)$	$\sigma_{\text{ph-i}} (10^{-21} \text{ cm}^2)$	$\sigma_{\text{ph-abs}} (10^{-19} \text{ cm}^2)$
275	0.073	0.51	0.091
310	74.6	300	86.4

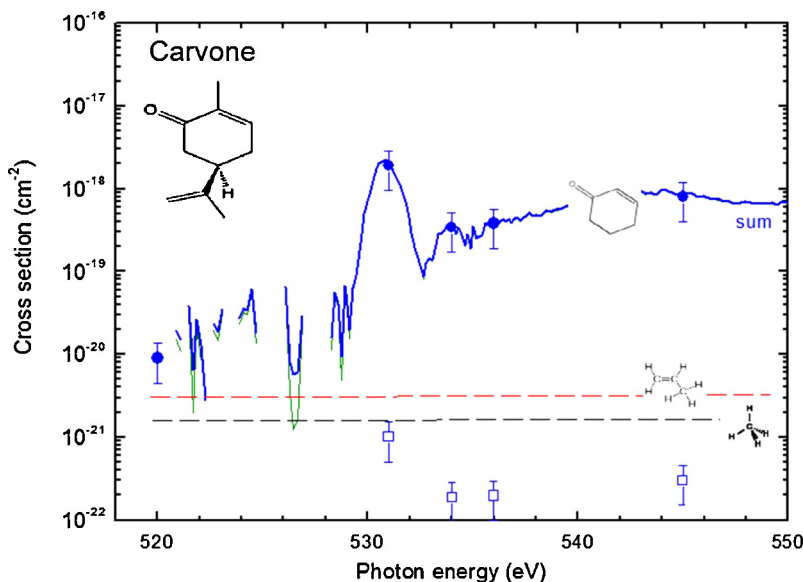


Fig. 11. Absorption cross section (lines) of selected molecules (e.g. methane, propene, 2-cyclohexenone) from COREX Database around O 1s edge. For methane and propane, it was employed the same absorption cross section value before the C 1s ionizing potential (~ 280 eV). The sum of these cross section is an approximation for the carvone absorption cross section around O 1s edge. Non-dissociative single ionization (photoionization) cross section ($\sigma_{\text{ph-i}}$) and dissociative ionization (photodissociation) cross section ($\sigma_{\text{ph-d}}$) of carvone as a function of photon energy are indicated by the circles and the squares, both with error bars, respectively.

Table 4

Non-dissociative single ionization (photoionization) cross section ($\sigma_{\text{ph-i}}$) and dissociative ionization (photodissociation) cross section ($\sigma_{\text{ph-d}}$) of carvone as a function of photon energy around the O 1s edge. Estimated values for absorption cross section ($\sigma_{\text{ph-abs}}$) of carvone are also listed. The estimated total error is 50%.

Photon energy (eV)	$\sigma_{\text{ph-d}}$ (10^{-19} cm 2)	$\sigma_{\text{ph-i}}$ (10^{-21} cm 2)	$\sigma_{\text{ph-abs}}$ (10^{-19} cm 2)
520	0.082	0.0036	0.091
531	17.3	0.91	19.1
534	3.1	0.18	3.5
536	3.5	0.18	3.82
545	7.2	0.27	8.0

The absorption cross section (lines) for methane, propene and 2-cyclohexenone, obtained from the COREX Database around the O 1s edge is presented in Fig. 11. For methane and propane, the same absorption cross section value obtained before the C 1s ionizing potential (~ 280 eV) was used. The sum of these cross sections is an approximation to the carvone absorption cross section around the O 1s edge. The single photoionization cross section and photodissociation cross section ($\sigma_{\text{ph-d}}$) of carvone as a function of photon energy are indicated by the circles and the squares, respectively. The estimated total error is 50%. These values as well the estimated values for the absorption cross section ($\sigma_{\text{ph-abs}}$) of carvone at 520 eV, 532 eV, 534 eV, 536 eV and 545 eV photon energy are listed in Table 3. The absorption cross section is approximately $0.1 \cdot 10^{-19}$ cm 2 at 275 eV and $95 \cdot 10^{-19}$ cm 2 at 310 eV and reaches a maximum value of $21 \cdot 10^{-19}$ cm 2 at 531 eV (close to the O 1s edge) (Table 4).

4. Conclusions

The mass spectra for the carvone molecule, obtained around the C 1s and O 1s edges, along with the total ion yield spectrum for this molecule, measured around the O 1s edge, have been reported for the first time. For the sake of comparison, the valence mass spectrum, obtained with a He I discharge lamp, has also been reported. At 21.21 eV, the carvone mass spectrum shows a high value for the parent ion [47.4%] branching ratio. At higher photon energies, around the C 1s and O 1s edges, fragmentation of the molecule

increases and the parent ion relative intensity decreases. At 275 eV and 310 eV, the base peak corresponds to the highly stable C₅H₆O⁺ ion [$m/z = 82$]. At higher photon energies [520–545 eV], the base peak corresponds to the C₃H₃⁺ [$m/z = 27$] ion and the parent ion is not observed. Atomization of the carvone molecule was observed at high photon energies as indicated by the production of C⁺, whose relative intensity increases from 310 eV to 520 eV.

Three well defined resonances are observed in the O 1s TIY spectrum, at: 531 eV, 534 eV and 536 eV photon energies. A broad structure is also observed at 545 eV. The first two resonance are probably associated, by analogy with the photoabsorption spectra of similar ketones, to pi-antibonding excitations, while the third involves a vacant atomic orbitals (3s and 3p) followed by Rydberg states. The broad structure may be related to a shape sigma-resonance, despite a strong controversy in the literature concerning this assignment. The main relaxation route following core-excitation around the O 1s edge involves the production of the H⁺ ion with high yields. Previously unreported fragments have been observed: H₃⁺, CH₂²⁺, O²⁺, O⁺, HO⁺ and H₂O⁺. The observation of atomic oxygen singly [O⁺] and doubly charged [O²⁺] points out to a site-selective fragmentation following the O 1s excitation. The relative intensities of O⁺ and O²⁺ are greatly increased near the O 1s edge, reaching a maximum at 536 eV. Absolute values for the photoabsorption cross sections have been estimated on both the C 1s and O 1s ionization edges, using the additive molecular rule.

Carvone may be considered as a prototype molecule for the study of the interaction of VUV photons with monoterpenes, chemical compounds commonly found in many plants. The carvone molecule may play a role in the eventual interaction of high energy photons with plants. We hope the present paper will contribute to the increase of experimental and theoretical work regarding the interaction of VUV photons with chemical compounds found in plants.

Acknowledgements

The authors would like to thank the Brazilian Synchrotron Facility (LNLS) for the technical and finance support for the experiments.

This work is partially supported by Brazilian Agencies CNPq and FAPERJ.

References

- [1] B.P. Tsai, J.H.D. Eland, *Int. J. Mass Spectrom. Ion Processes* 36 (1980) 143.
- [2] R.G. Kingston, M. Guilhaus, A.G. Brenton, J.H. Beynon, *Org. Mass Spectrom.* 20 (1985) 406.
- [3] W. Eberhardt, T.K. Sham, R. Carr, S. Krummacher, M. Strongin, S.L. Weng, D. Wesner, *Phys. Rev. Lett.* 50 (1983) 1038.
- [4] G.G.B. de Souza, P. Morin, I. Nenner, *Phys. Rev. A* 34 (1986) 4470.
- [5] A.P. Hitchcock, J.J. Neville, in: T.K. Sham (Ed.), Part I: Dynamics and VUV Spectroscopy, Advanced Series in Physical Chemistry, vol. 12A, World Scientific, Singapore, 2002, pp. 154–227 (Chapter 4).
- [6] D.M. Hanson, *Advances in Chemical Physics*, vol. 77, Wiley, 1990, pp. 1–38.
- [7] C. Miron, P. Morin, in: M. Quack, F. Merkt (Eds.), *Handbook of High-resolution Spectroscopy*, vol. 3, John Wiley & Sons Ltd., Chichester, UK, 2013, pp. 1665–1690.
- [8] A.F. Lago, L.H. Coutinho, R.R.T. Marinho, A.N. de Brito, G.G.B. de Souza, *Chem. Phys.* 307 (2004) 9.
- [9] L.H. Coutinho, M.G.P. Homem, R.L. Cavasso-Filho, R.R.T. Marinho, A.F. Lago, G.G.B. de Souza, A.N. de Brito, *Braz. J. Phys.* 35 (4) (2005) 940.
- [10] S. Pilling, A.F. Lago, L.H. Coutinho, R.B. de Castilho, G.G.B. de Souza, A.N. de Brito, *Rapid. Commun. Mass Spectrom.* 21 (2007) 3646.
- [11] G.G.B. de Souza, L.H. Coutinho, C.V. Nunez, R. Bernini, R.B. de Castilho, A.F. Lago, *J. Phys. Conf. Ser.* 88 (2007) 012005.
- [12] R.B. de Castilho, C.V. Nunez, L.H. Coutinho, A.F. Lago, R.B. Bernini, G.G.B. de Souza, *J. Electron Spectrosc. Relat. Phenom.* 155 (2007) 77.
- [13] G. Martins, A.M. Ferreira-Rodrigues, G.G.B. de Souza, N.J. Mason, S. éden, D. Duflot, J.P. Flament, S.V. Hoffmann, J. Delwiche, M.J. Hubin-franskin, P. Limão-Vieira, *Phys. Chem. Chem. Phys.* 11 (2009) 11231.
- [14] K.K. Aggarwal, S.P.S. Khanuja, A. Ahmad, T.R.S. Kumar, V.K. Gupta, S. Kumar, *Flav. Frag. J.* 17 (2002) 59.
- [15] R. Karousou, G. Grammatikopoulos, T. Lanaras, Y. Manetas, S. Kokkini, *Phytochemistry* 49 (1998) 2273.
- [16] T. Egawa, Y. Kachi, T. Takeshima, H. Takeuchi, S. Konaka, *J. Mol. Struct.* 658 (2003) 241.
- [17] E. von Sydow, *Acta Chem. Scand.* 18 (1964) 1099.
- [18] G.A. Garcia, L. Nahon, I. Powis, *Int. J. Mass Spectrom.* 225 (2003) 261.
- [19] C.J. Harding, I. Powis, *J. Chem. Phys.* 125 (2006) 234306.
- [20] C.J. Harding, E. Mikajlo, I. Powis, S. Barth, S. Joshi, V. Ulrich, U. Hergenhahn, *J. Chem. Phys.* 123 (2005) 234310.
- [21] S. Pilling, D.P.P. Andrade, R. Neves, A.M. Ferreira-Rodrigues, A.C.F. Santos, H.M. Boechat-Roberty, *Mon. Not. R. Astron. Soc.* 375 (4) (2007) 1488.
- [22] M. Simon, T. Lebrun, R. Martins, G.G.B. de Souza, I. Nenner, M. Lavallee, P. Morin, *J. Chem. Phys.* 97 (1993) 5228.
- [23] F. Burmeister, L.H. Coutinho, R.R.T. Marinho, M.G.P. Homem, M.A.A. de Moraes, A. Mocellin, O. Björnholm, S.L. Sorensen, P.T. Fonseca, A. Lindgren, A. Naves de Brito, *J. Electron Spectrosc. Relat. Phenom.* 180 (2010) 6–13.
- [24] H.Y. Afefy, J.F. Liebman, S.E. Stein, in: P.J. Linstrom, W.G. Mallard (Eds.), *NIST Chemistry WebBook*, National Institute of Standards and Technology, Gaithersburg, MD, 2005, NIST Standard Reference Database Number 69 <http://webbook.nist.gov>
- [25] A.P. Hitchcock, C.R. Brion, *J. Electron. Spectr.* 18 (1980) 1.
- [26] D. Duflot, J.P. Flament, I.C. Walker, J. Heinesch, M.J. Hubin-Franskin, *J. Chem. Phys.* 118 (2003) 1137.
- [27] I. Ishii, A.P. Hitchcock, *J. Electron Spectrosc. Relat. Phenom.* 46 (1988) 55.
- [28] A.P. Hitchcock, D.C. Mancini, COREX DATABASE, *J. Electron Spectrosc. Relat. Phenom.* 67 (1) (1994) <http://unicorn.mcmaster.ca/corex/cedb-title.html>
- [29] M.H. Chen, B. Crasemann, H. Mark, *Phys. Rev. A* 24 (1981) 177.
- [30] H.M. Boechat-Roberty, S. Pilling, A.C.F. Santos, *Astr. Astrophys.* 438 (2005) 915.
- [31] S. Pilling, A.C.F. Santos, H.M. Boechat-Roberty, *Astr. Astrophys.* 449 (2006) 1289.
- [32] F. Fantuzzi, S. Pilling, A.C.F. Santos, L. Baptista, A.B. Rocha, H.M. Boechat-Roberty, *Mon. Not. R. Astron. Soc.* 417 (2011) 2631.
- [33] S. Pilling, A.C.F. Santos, H.M. Boechat-Roberty, G.G.B. de Souza, *J. Electron Spectrosc. Relat. Phenom.* 155 (2007) 70.
- [34] A.H.A. Gomes, W. Wolff, N. Ferreira, K.F. Alcantara, H. Luna, G.M. Sigaud, A.C.F. Santos, *Int. J. Mass Spectrom.* 319–320 (2012) 1.
- [35] S. Pilling, R. Neves, A.C.F. Santos, H.M. Boechat-Roberty, *Astr. Astrophys.* 464 (2007) 393.
- [36] G. Cooper, M. Gordon, D. Tulumello, C. Turci, K. Kaznatcheev, A.P. Hitchcock, *J. Electron Spectrosc. Relat. Phenom.* 137–140 (2004) 795.
- [37] H.M. Boechat-Roberty, R. Neves, S. Pilling, A. Lago, G.G.B. de Souza, *Mon. Not. R. Astron. Soc.* 394 (2009) 810.